Acid generation potential and kinetics of metal(loid) release from resuspended sulfidic mine waste

Jillian Helser[a,b], Valérie Cappuyns[a,b]

[a] KU Leuven, Department of Earth and Environmental Sciences, 3001 Leuven, Belgium

[b] KU Leuven, Research Center for Economics and Corporate Sustainability (CEDON), 1000 Brussels, Belgium

Corresponding Author:

Jillian Helser

KU Leuven, Department of Earth and Environmental Sciences

Celestijnenlaan 200E- Box 2411

3001 Leuven, Belgium

Email: valerie.cappuyns@kuleuven.be

Acid generation potential and kinetics of metal(loid) release from resuspended sulfidic mine waste

Jillian Helser [a,b], Valérie Cappuyns[a,b]

Abstract

Sulfidic mine waste exposed to oxidizing conditions can generate acidity and leach metal(loid)s into the environment, posing a risk to surrounding ecosystems. In the present study, four sulfidic mine waste samples were investigated using both kinetic and static experiments to determine the acid generation potential and mobilization of metal(loid)s. A long-term resuspension experiment of 821 days was performed to study the effect of oxidation on the acid generation and the release of metal(loid)s from the mine waste samples. The mineralogy of the mine waste after 821 days of oxidation was determined and compared with the original sample. A kinetic study of a pH-dependent leaching test was also performed to study the influence of time on metal(loid) release. Additionally, a static acid-base accounting test was used to gain more insight into the acid generation and neutralization potentials. The mineralogical study revealed the presence of sulfide minerals (e.g., pyrite, and sphalerite) both as free particles and embedded within other minerals (e.g., quartz). The mine waste samples exhibited a high acid generation potential, where the pH of all samples decreased to pH<3 after 272 days. The resuspension of the mine wastes also resulted in a considerable release of As, Cd, Cu, and Zn (up to 4,500, 100, 4,000, and 11,500 mg/kg, respectively). However, Pb exhibited low leaching levels, due to the formation of secondary Pb-bearing minerals (i.e., beudantite and/or plumbojarosite). Overall, the samples pose an environmental risk based on the high acid generation potential and high release of metal(loid)s.

Keywords: Resuspension; leaching; mineral oxidation; potentially toxic elements; acid generation; extractive waste

1. Introduction

Large amounts of mine wastes generated from mining and mineral processing commonly contain high concentrations of potentially toxic elements, which are bound primarily to sulfide minerals [1]. Sulfides exposed to oxidizing conditions may result in the generation of acid mine drainage (AMD) with low pH and release of sulfates and metal(loid)s. In some cases, the presence of acid-neutralizing minerals can reduce the AMD generation potential.

The main acid-generating sulfide species include Fe-sulfides, such as pyrite (FeS_2) and pyrrhotite ($Fe_{(1-x)}S$) and the most common acid-neutralizing minerals consist of relatively fast-reacting carbonates, such as dolomite ($CaMg(CO_3)_2$) and calcite ($CaCO_3$) and slower reacting silicates (e.g., mica and chlorite) [2–4]. However, some carbonate minerals, such as some Fe-carbonate minerals like siderite ($FeCO_3$), can be net acid-producing [4,5].

AMD is detrimental to the environment, for example, it can cause revegetation failures and pollute waterways. Different remediation and management techniques have been applied [6], such as dry cover (e.g., covering with soil or cement) or wet cover, two common techniques used in the remediation of mine waste to prevent sulfide oxidation [6,7]. A wet cover entails submerging the mine tailings under a water cover to curtail the issue of acid mine drainage by reducing the supply of oxygen to the sulfide minerals [8].

However, if mine waste is stored with a shallow wet cover, water agitation (e.g., waves from strong winds, boats, or addition of new tailings) could promote the resuspension of the tailings and the diffusion of

dissolved oxygen, resulting in the undesired generation of AMD [9,10]. Another possible scenario is the erosion of tailings causing particles to end up in water bodies and rivers. Experimental resuspension tests, in which mine waste is suspended in water, can mimic the abovementioned scenarios. Some studies [9,11,12] have performed different types of resuspension tests on mine wastes and sediments for varying durations (up to 840 days for mine waste, 11 days for sediments). However, longer-term leaching tests (>100 days) on mine waste are still rarely performed [13].

While the long-term resuspension test is a kinetic test that can provide more accurate insights into the acid production potential (APP) of the mine waste, other short-term static characterization methods exist. The most commonly used static APP prediction tests are acid-base accounting (ABA) tests which are typically lower in cost compared to kinetic tests [4]. ABA tests entail determining the sulfur/sulfide content of waste rock/tailing materials to calculate the acid potential (AP) and determining the neutralization potential (NP). There are many different variations of the ABA test, such as the Sobek method [14], the modified ABA [15,16], and the EU standard, based on the total carbon content [17]. While these tests are commonly employed [18,19], there are still various disadvantages of ABA tests, as outlined by Dold (2017) and Karlsson et al. (2018) [4,5]. For example, the NP of silicate minerals seems to be underestimated by laboratory experiments. Utilizing strong acids can cause an overestimation of the NP [4,5]. Furthermore, these static ABA tests do not indicate the source minerals of the NP and AP [20]; Therefore, some authors [20–22] have proposed some mineralogical-based approaches [4] to estimate the APP.

AMD generation prediction is difficult because it depends on various mineralogical, chemical, hydrological and microbiological factors (e.g., sulfur-oxidizing bacteria) [4,23,24]. Therefore, ABA tests should only be seen as a very simple, rough approach to attempt to quantify the AMD susceptible mineralogy through the use of geochemical data [5].

Additionally, ABA does not provide information on the rate at which sulfides oxidize [9,25]. Many studies have reported that metal(loid) release from extractive waste is time-dependent [13,18,26,27] and that acid generation potential depends on the rate at which the sulfides oxidize [9,25]. In order to evaluate the information obtained by ABA in comparison with longer-term oxidation, in the present study, a long-term kinetic resuspension test (>2 years) was performed in combination with a static ABA test [17], and mineralogical and chemical characterization of mine waste (tailings and waste rock) from historical and operational mining sites. The long-term resuspension test, perfomed toto study the kinetics of oxidation, included a mineralogical characterization of the mine waste before and after the resuspension experiment . The influence of pH on the release of metal(loid)s, and associated changes in mineralogical composition was also investigated. Kinetics of a pH-dependent leaching test was also accounted for. A 16S rRNA gene-based microbiome analysis was also performed on the mine waste before and after the resuspension tests to determine the role of microbial activity on the acid production and metal(loid) release. Since the mineralogical composition is key in studying AMD generation potential, mineralogical-based AMD calculations were also made (using mineralogical data from XRD and SEM measurements) and compared with the static ABA test.

2. Methodology

2.1 Samples

The sulfidic mine waste samples originated from two different sites in Europe: an operational mine Cu-Zn mine in Neves-Corvo, Portugal and a historical Cu-Pb-Zn mine in Freiberg, Germany. The studied samples consisted of fresh waste rock (NC_1), tailings (NC_2) and stored waste rock (NC_3) from Neves-Corvo and tailings (FR_1) from Freiberg. The studied samples were previously characterized in detail in Helser et

al. (2022) [28]. The mineralogy is presented in Table 1. The moisture content of each sample was determined according to ISO 11465 (1993) [29]. The resuspension tests were performed using the fresh tailings and waste rock samples, before drying or mechanically processing the samples. The grain size distribution was determined previously for the mine waste samples in Helser et al. (2022) [28]. In which 99% of both tailings samples NC_1 and FR_1 were <500 µm and 35 and 25% of waste rock samples NC_1 and NC_2 were larger than 500 µm, respectively [28]. For the EN 15875 test (static test for determination of acid potential and neutralization potential of sulfidic waste, EN 15875 (2011)[17]), the samples were sieved and ground to 95% <0.125 mm, as required by the protocol. For the pH-dependent leaching test, the samples were dried (<45°C) and ground to <500 µm.

2.2 Mineralogical and chemical characterization

The mineralogy of the mine wastes after the resuspension experiment was determined using X-ray diffraction (XRD; Philips PW1830 diffractometer with Bragg/Bretano θ-2θ setup, CuKα radiation, 45 kV and 30 mA, graphite monochromator) and compared with the mineralogy of the original samples determined by Helser et al. (2022) [28]. An internal standard of 10 wt% ZnO was added to the residues for quantitative mineralogical analysis. The mineral phases were identified with Profex 4.0 software using the Rietveld refinement method [30,31]. The detection limit was manually set to 0.5 wt%.

Scanning electron microscopy (SEM) results for sample NC_1 were presented in Helser et al. (2021) [32]. Punctual microanalyses were made on polished sections of large grains (>2 cm) and fine powder from fresh waste rock sample NC_1 using SEM with energy-dispersive X-ray spectroscopy (EDS) for backscattered electron images and compositional information. A scanning electron microscope JEOL 6400 was used under high vacuum conditions (10^{-4} Pa) and with up to 300,000 magnifications. It was coupled with an energy dispersive X-ray microanalysis system (EDS Oxford-INCA) with a Si(Li) window-less detector. A vacuum evaporator (JEOL JEE-4X) was used for the preparation of the polished sections.

2.3 Resuspension experiment

Resuspension experiments were performed on all four samples, i.e., NC_1, NC_2, NC_3 and FR_1, for 821 days. Additionally, a short-term resuspension test was performed on sample FR_1 for 2 weeks (mineralogical comparison of residue in Supplementary Table S1). Deionized water was added to a predetermined amount (based on the moisture content) of fresh/wet sample in a 1 liter Erlenmeyer flask at a liquid-to-solid (L/S) ratio of approximately 10 L/kg. The slurry was constantly agitated on a rotary shaker at 125 rpm. Deionized water was constantly added to the slurry to maintain a constant L/S ratio. Approximately 6 ml liquid aliquots were taken periodically (0 h, 1.5 h, 4 h, 1 d, 2 d, 3 d, 4 d, 9 d, 10 d, 11d, 14 d, 15 d, 16 d, 17 d, 18 d; then, once every 3 days until 2 months; then, once a week until 6 months, and once a month until 821 days). To take samples, the shaker was stopped, and once the particles were slightly settled, a plastic tube (length: ~200 mm; width: ~3mm) attached to a syringe and a 0.45µm Chromafil® PET45/25 filter were used to draw up the leachate. The soluble elements in the leachates were determined with inductively coupled plasma optical emission spectrometry (ICP-OES, Varian/Agilent 720-ES). Prior to ICP-OES analyses, the leachates were acidified to pH<2 with ultrapure HNO_3 and stored at 5-10°C. Additionally, the pH, electrical conductivity (EC) and redox potential (Eh) of the leachates were measured using Eijkelkamp (The Netherlands) equipment. One ml aliquots, collected in the same way as the liquid aliquots for ICP-OES analysis, were stored at approximately -17°C before analyses of the sulfate content with ion chromatography (IC; Dionex ICS-2000, Thermo Scientific). The concentrations of leached elements were compared with the (pseudo)-total concentrations determined via aqua regia digestion (HCl/HNO_3, 3:1 solution) or X-ray fluorescence (XRF) by Helser et al. (2022) (Supplementary Table S2).

2.4 16S rRNA gene-based microbiome analysis

The CTAB (cetyltrimethylammonium bromide) DNA extraction technique performed was adapted from Larsen et al., (2007). First, 1800 µL of the aqueous sample was taken from each well-mixed Erlenmeyer flask and transferred to a 2 ml centrifuge tube. Then, approximately 2 g of solid (mine waste) sample were initially taken from each flask using a spoon long enough to reach the mine waste particles at the bottom of the flask. A representative sample of approximately 0.25 g was weighed from the initial 2 g sample. The original samples were also analyzed (in duplicates), 0.25 g (slightly more for the slurry sample, NC_2, due to the excess water content) of each sample were weighed in a 2 ml microcentrifuge tube.

Aqueous samples were first centrifuged for 10 min at 2000 x g (g-force) and then the supernatant was discarded. The remaining cell pellet was suspended in 450 µL of GTE (Glucose, Tris.Cl, and EDTA) solution. The 12 solid samples (4 aqueous leachates, 4 original solid mine waste samples and 4 solid mine waste residues, after 685 days of resuspension) were directly suspended in 450 µL of the GTE solution without the need for centrifugation. Then, 50 µL of a 10 mg/mL lysozyme solution was added to each centrifuge tube, mixed gently and incubated overnight at 37°C. Then, 150 µL of a 2:1 solution of 10% sodium dodecyl sulfate (SDS) and 10 mg/mL of proteinase K was added, mixed gently, and incubated for 30 min at 55°C. After, 200 µL of 5 M NaCl was added to block the binding of DNA to the cetrimide and mixed gently. Then 160 µL of CTAB (sodium chloride and cetrimide) solution (preheated at 65°C) was added, gently mixed and incubated for 10 min at 65°C. Then, approximately 800 µL of a 24:1 (v/v) solution of chloroform/isoamyl alcohol was added, shaken vigorously, and centrifuged for 5 min at 15000 rpm. The aqueous layer was transferred to a new 2 mL centrifuge tube. The extraction with the chloroform/isoamyl alcohol solution was repeated and the aqueous phase was again transferred to a new centrifuge tube. Then, 560 µL of isopropanol was added, mixed gently to precipitate the DNA, incubated for 5 min at room temperature, centrifuged for 10 min at 15000 rpm, and then the supernatant was discarded. The remaining DNA pellet was washed with 1 ml of 70% ethanol, mixed gently and centrifuged for 10 min. The supernatant was carefully discarded and the remaining DNA pellet was washed again, but with 200 µL of 100 % ethanol, gently mixed and centrifuged for 5 min. The supernatant was carefully discarded and the DNA pellet was dried at 35°C until the liquid evaporated. 20 µL of nuclease-free water was added to the dried DNA pellet, vortexed, centrifuged and stored overnight at room temperature to allow the pellet to dissolve. Then, the samples were stored in the freezer until further analysis.

2.5 Acid-base accounting (ABA) test

The European Committee for standardization (CEN)'s static test for the determination of acid potential (AP) and neutralization potential (NP) of sulfidic waste (EN 15875, 2011; [17]) was performed on the mine waste samples. Briefly, 2 g (dry mass) of sample and 90 mL of deionized water were added to a 250 mL graduated cylinder and mixed with a magnetic stirrer (Hanna Instruments HI 190M). First, the pH of the slurry was measured at t=0 h and then 1 mol/L HCl was added. The amount of HCl added was based on the carbonate content of the samples, which was determined based on their mineralogical data (XRD). The mixture was covered and left stirring overnight. After 22 h, the pH (Eijkelkamp, The Netherlands) was measured: if the pH was <2, the experiment was restarted with a lower initial addition of HCl; if the pH was >2.5, extra HCl was added. Then, at t=24 h, 100 mL of deionized water was mixed with the sample and solution and the pH was measured. If the pH was not between 2 and 2.5 the experiment was restarted. Then, the mixture was back titrated using 0.1 mol/L NaOH until reaching a pH of 8.3. The amounts of HCl and NaOH added were recorded to calculate the NP (in carbonate equivalents in kg/t). The AP (in carbonate equivalents in kg/t) was determined by multiplying the total sulfur content by a conversion factor of 31.25. The net neutralization potential (NNP, carbonate ($CaCO_3$) equivalents in kg/t) was calculated as [17]:

$$NNP=NP-AP \quad (1)$$

For comparison with the static laboratory test [17] NNP values, mineralogical NNP values were also determined using theoretical calculations based on mineralogy (XRD results) according to Karlsson et al. (2018) and Dold (2017).

2.6 pH-dependent leaching test kinetics

A pH-dependent leaching test (modified CEN/TS 14429 or modified US EPA method 1313) was performed on mine tailing sample NC_2, with varying shaking times to evaluate the effect of time on the release of metal(loid)s at different pH values. The test was performed at four different durations (2, 6, 24, 48 h) with seven different extraction fluids with varying concentrations of HNO_3 or NaOH: pH 0.5 (0.3 mol/L HNO_3), 1 (0.1 mol/L HNO_3), 2 (10^{-2} mol/L HNO_3), 3 (10^{-3} mol/L HNO_3), 11 (10^{-3} mol/L NaOH), 13 (0.1 mol/L NaOH) and neutral pH (~7) with ultrapure water (Milli-Q®). The extraction fluid was added to the dried and ground sample (particle size < 500 µm) at an L/S ratio of 10 L/kg and shaken at 100 rpm on a reciprocal shaker. The final pH was measured using an Eijkelkamp (The Netherlands) pH meter and supernatants were filtered using a syringe and a 0.45µm Chromafil® PET45/25 filter. The leachates were stored in the refrigerator at 5–10°C until ICP-OES analysis.

2.7 Quality control

In all tests, at least one procedural blank was included in each batch. The pH-dependent leaching test and acid-base accounting test were performed in duplicates. Additionally, all chemicals and acids used during the experiments were analytical and ultrapure grade, respectively. For elemental analyses with ICP-OES, Al, As, Ba, Ca, Cd, Co, Cru, Cu, Fe, K, Mg, Mn, Mo, Na, Ni, P, Pb, S, Sb, Sr, V and Z were analyzed from one single run with 3 replicates, 5 s each.

2.8 Geochemical modeling

The PHREEQC geochemical software [34][34] and phreeqc.dat were used to model the kinetic oxidation of pyrite simulating conditions similar to the resuspension experiment (L/S ratio of 10 L/kg) considering an initial abiotic environment. Both the oxidation of pyrite by molecular oxygen or ferric iron were considered. The rate expressions of pyrite oxidation were defined based on the following equations [35,36]:

oxidation by O_2:

$$r = 10^{-8.19} m_{O_2}^{0.5} O_2 m_{H^+}^{-0.11} \quad (2)$$

oxidation by Fe^{3+} and in the presence of O_2:

$$r = 6.3\ x\ 10^{-4} m_{Fe^{3+}}^{0.92} (1 + m_{Fe^{2+}}/10^{-6})^{-0.43} \quad (3)$$

and oxidation by Fe^{3+} without oxygen:

$$r = 1.9\ x\ 10^{-6} m_{Fe^{3+}}^{0.28} (1 + m_{Fe^{2+}}/10^{-6})^{-0.52} m_{H^+}^{-0.3} \quad (4)$$

Where r is the rate of pyrite oxidation in mol/m^2/s and m is the concentration (molality). The rates (r) in Equations 2-4 are multiplied by the initial surface area (m^2) and concentration (g/L) of pyrite to obtain the reaction in mol/L/s [36].

The initial surface area of pyrite, A_0, was estimated using the following equation [37]:

$$A_0 = \frac{2[(ab) + (bc) + (ac)]}{(abc)\ x\ \rho} \quad (5)$$

where ρ is the density of pyrite (5.01 g/cm^3; [36]) and a, b and c are the dimensions of the particle. The pyrite grains are assumed to be cubic shaped [37] and based on a grain size of 500 µm.

Additionally, the input parameters include oxygen (8 mg/l), ambient temperature (25°C) and the pH of the original mine waste sample (e.g., pH 5.4 for NC_2) as the initial pH value.

The solubility products for plumbojarosite ($K_{sp}=10^{-16.28}$) and beudantite ($K_{sp}=10^{-15}$) were from [38] and [39], respectively.

3. Results and Discussion

3.1 Mineralogical and chemical sample characterization

The original mine waste samples were characterized by high levels of As, Cd (especially tailings samples NC_2 and FR_1), Cu, Pb (especially tailings samples NC_2 and FR_1), Sb (sample NC_2) and Zn (Supplementary Table S2; [28]).

The original mine wastes contained potentially acid-generating minerals such as (As-) (Cu-) pyrite and sphalerite ((Zn, Fe)S). Sphalerite can be oxidized by either dissolved molecular oxygen (O_2) or Fe(III), but only the latter process produces acidity. However, sphalerite is commonly considered to be non-acid producing because, if Fe(III) has been produced by oxidation of Fe(II), there is no net effect on acidity [40]. The original mine waste samples also contained potentially acid-neutralizing minerals such as dolomite ($CaMg(CO_3)_2$) and hydrotalcite ($Mg_6Al_2CO_3(OH)_{16}{\cdot}4(H_2O)$) (Table 1). Additionally, all samples originally contained siderite ($FeCO_3$), which can be both acid-neutralizing as well as acid-generating [5].

XRD is known to be more accurate in measuring large and abundant crystalline structures rather than small and minor structures. Thereby, it is likely that other minerals that occur in very minor amounts or small crystalline phases may also be present, which were not detected by XRD in some samples, such as galena (PbS), sphalerite (Fe, Zn)S), cerussite ($PbCO_3$) and arsenopyrite [41].

The SEM-EDS images of three polished sections of selected particles of waste rock sample NC_1 are shown in Supplementary Figures S1-S5. The fine powder sample (NC_1_A) was composed of ankerite, pyrite, calcium and clay minerals. One of the larger particle waste rock samples (NC_1_B) contained pyrite encapsulated in quartz, as well as chalcopyrite, mica, biotite, rutile and zircon. The other larger particle sample (NC_1_C) contained quartz veining with Fe-oxides, calcium sulfate, calcite and a mixture of clay and sulfate minerals.

3.2 Resuspension experiment

The original samples contained high concentrations of pyrite (2-35 wt%; Table 1), a key mineral in acid mine drainage generation [28]. Pyrite was still found in samples NC_1, NC_2, and FR_1 after 821 days of resuspension (Table 1). In all cases except NC_1, there was a decrease in pyrite after resuspension compared to the original mine waste by at least 1 wt%. After resuspension of the mine waste samples, siderite completely dissolved from all samples, sphalerite ((Zn, Fe)S), chalcopyrite ($CuFeS_2$), arsenopyrite (FeAsS), and dolomite were also no longer detected in sample FR_1. Note that the total amount of quartz does not increase. Its relative amount increases because of the dissolution of other minerals (e.g., siderite, sphalerite, etc.).

Interestingly, the formation of Pb-bearing minerals, either beudantite ($PbFe_3(OH)_6SO_4AsO$) and/or plumbojarosite ($PbFe_6(SO_4)_4(OH)_{12}$), was observed in samples NC_1, NC_2 and FR_1 (1-3 wt%) by the end of the 821-day resuspension experiment. Beudantite is generally formed by the release of As, Fe, and Pb from the oxidation of galena (PbS) and arsenopyrite [39,42] and is stable under acidic and oxidant conditions [43]. Plumbojarosite is also expected to be stable under acidic conditions [44].

Table 1 Mineralogy of original mine waste samples from Helser et al. (2021) (left) and after the resuspension experiments of 821 days (right).

		Original samples				After 821 d resuspension			
Mineralogy (wt%)	Formula	NC_1	NC_2	NC_3	FR_1	NC_1	NC_2	NC_3	FR_1
Quartz	SiO_2	36	25	35	38	45	41	40	47
Feldspars					5				6
Clay minerals/Micas		36	14	38	15	30	14	42	18
Pyrite	FeS_2	5	35	2	13	5	25		12
Chalcopyrite	$CuFeS_2$				1				
Arsenopyrite	FeAsS				1				
Clinochlore	$Mg_6Si_4O_{10}(OH)_8$		4	6			5	5	
Chlorite	$(Mg,Fe)_3(Si,Al)_4O_{10}(OH)_2 \cdot (Mg,Fe)_3(OH)_6$	18	18	10	12	18	12	5	8
Rutile	TiO_2	2	1	2				2	
Dolomite	$CaMg(CO_3)_2$				4				
Hematite	Fe_2O_3				2				2
Hydrotalcite	$Mg_6Al_2CO_3(OH)_{16} \cdot 4(H_2O)$	1	2	2	3			1	4
Gypsum	$CaSO_4.2H_2O$			5				5	
Siderite	$FeCO_3$	3	2	1	6				
Sphalerite	ZnS				1				
Beudantite / Plumbojarosite	$PbFe_3(OH)_6SO_4AsO_4$ / $PbFe_6(SO_4)_4(OH)_{12}$					1	3		2

The pH dropped significantly over time (Figure 1). The samples started with a pH of 3.5-6.1, followed by a quick decrease in pH reaching a pH value < 2.5 for all samples by the final measurement (day 821). The acid generation potential and metal(loid) release from the oxidation of mine waste can depend on different biological, chemical and physical factors. For example, the presence of acid-producing (e.g., (arseno-), (chalco-) pyrite) or acid neutralizing minerals (e.g., carbonate minerals) and their dissolutions plays a key role in the evolution of pH and metal(loid) release. Thereby, the mineralogy and microbial activity of the mine waste materials before and after oxidation are investigated in relation to the acid production and metal(loid) and sulfur release. The 16S rRNA gene-based microbiome analysis revealed low (below detection limit) to no microbial activity before or during resuspension of the mine waste; thereby, chemical oxidation is likely the main contributor to the acid generation and associated metal(loid) release.

Some studies have reported that mine tailings can be challenging environments for microorganisms to survive because they are characteristically oligotrophic environments and loaded with toxic metal(loid)s [45–47].

The variation of electrical conductivity (EC) as a function of time during the resuspension tests is shown in Supplementary Figure S6 for each sample. An inverse relation was seen between the EC measurements and the pH. The initial EC values were 0.97 mS/cm, 1.35 mS/cm, 4.73 mS/cm and 552 µS/cm for samples NC_1, NC_2 and NC_3, and FR_1, respectively. On day 430 the EC was 6.98, 19.8, 12.5, and 8.48 mS/cm for samples NC_1, NC_2 and NC_3, and FR_1, respectively; and by day 821 it increased to 7.76, 24.1, 10.6, and 13.7 mS/cm, respectively.

The initial redox potentials (Eh) of samples NC_1, NC_2, NC_3 and FR_1 were 307, 284, 395 and 347 mV, respectively and increased throughout the experiment (Supplementary Figure S7). From day 703 to the final day (day 821), the Eh increased from 566 to 625 mV, 574 to 616 mV, 645 to 672 mV, and 580 to 629 mV on day 703 to day 821 for samples NC_1, NC_2, and NC_3, and FR_1, respectively.

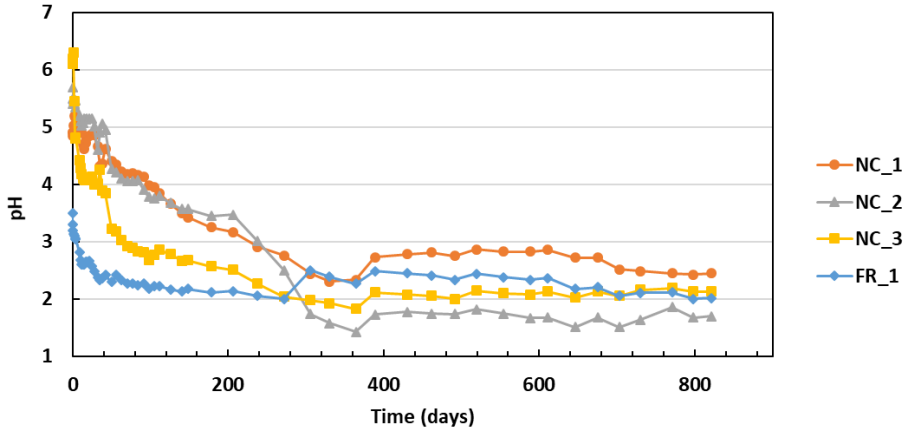

Figure 1 Variation of solution pH during the resuspension tests of samples NC_1, NC_2, NC_3 and FR_1.

There was a high release of metal(loid)s during the resuspension tests (Figure 2), especially from the Neves-Corvo tailings sample (NC_2), with up to 100% (equivalent to 4,000 mg/kg) of As in the sample leached. While the percentage of the total As released for the other samples is lower (<20%), there is still 0.2-200 mg/kg of As leaching. Additionally, there was a relatively high release of Cd (56-100% of the total Cd concentrations, 2-105 mg/kg), Cu (47-68% of the total Cu concentrations, 487-2,400 mg/kg), and Zn (64-100% of the total Zn concentrations, 743-10,000 mg/kg) from all samples. In some cases, there were fluctuations in the percentages leached of certain metal(loid)s. For example, 100% of As from sample NC_2 was leached around day 400, followed by a fluctuation in the As concentrations until day 821, whereafter, the As concentrations decreased, likely due to precipitation or readsorption.

Overall, Pb had an extremely low leaching efficiency, with less than 2% released of the total concentrations for all samples. Additionally, less than 50% of Fe was leached, with sample NC_2 having the highest release (50%, 132,000 mg/kg). Sample NC_3 (88%), had the highest percentage of sulfur release, followed by NC_2 (51%), FR_1 (33%) and NC_1 (23%). However, in terms of the sulfur concentrations released, NC_2 had the highest leached concentration (130,000 mg/kg) followed by FR_1 (44,000 mg/kg), NC_3 (24,000 mg/kg) and NC_1 (17,000 mg/kg).

Sulfate results from IC analysis are in agreement with the sulfur concentrations measured by ICP-OES for selected samples (t= 0.17, 21, 50, 98, 430, and 821 days. The detailed comparison can be found in Supplementary Table S3, showing that the majority/all of the present soluble sulfur is in the form of sulfate.

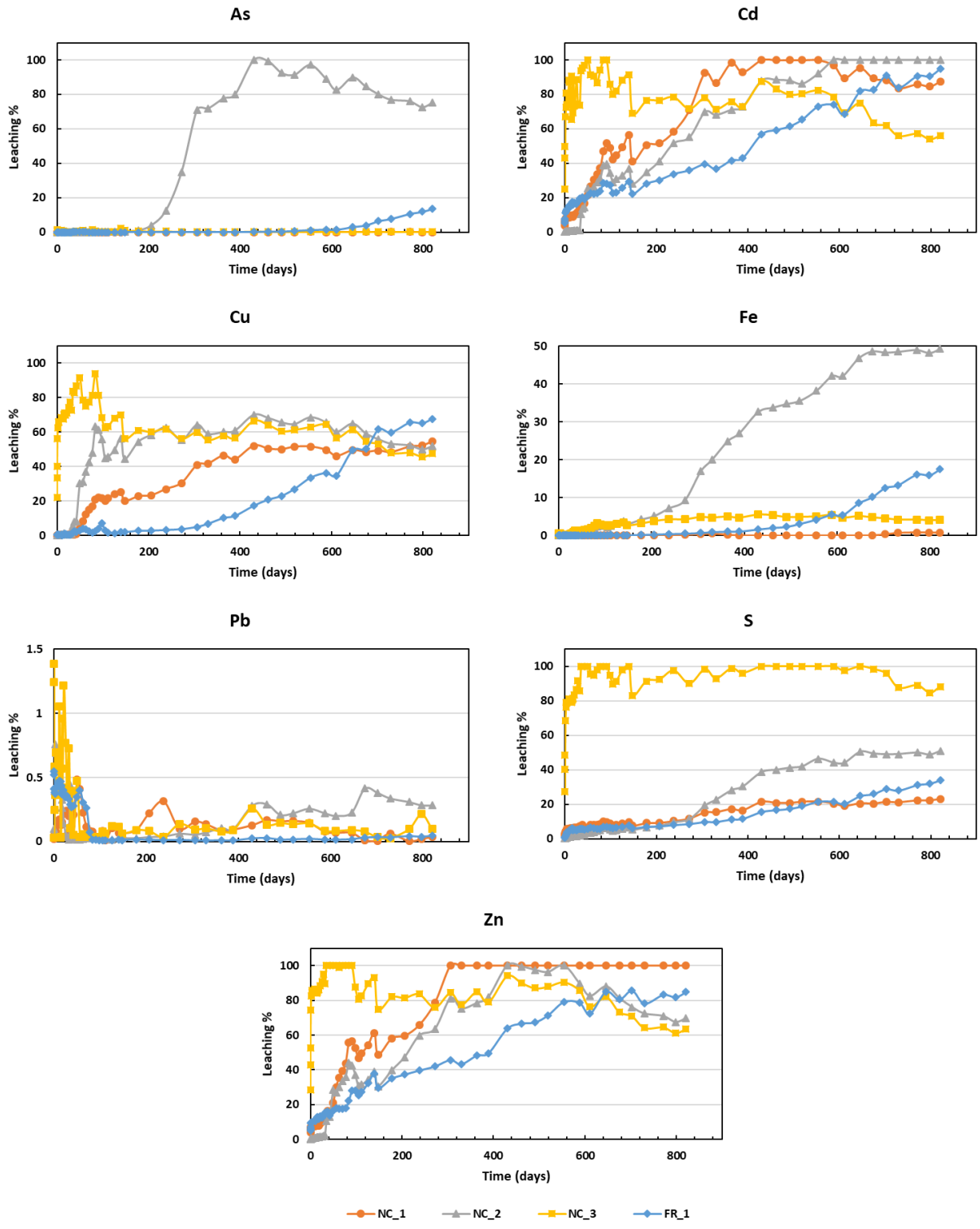

Figure 2 Percentage of metal(loid)s and S release over time during the resuspension experiments. Amount released is a percentage of the total concentrations, which is determined based on aqua regia digestion/XRF.

Additionally, the pyrite content only varied slightly from the original sample FR_1 (12 wt% of pyrite) compared to after the 2-week resuspension experiment (9 wt%) and the 821-day sample (12 wt%) (Supplementary Table S1). Little to no pyrite dissolved from sample FR_1 during the resuspension experiments. Some slight variations in the mineralogy could occur due to the small subsample of the fresh wet tailings, which might not be representative of the whole sample.

3.2.1 Oxidation of (Arseno-, Chalco-) Pyrite

The high acid generation potential is mostly attributed to the high pyrite content amongst the samples (2-35 wt%, Table 1). One mole of pyrite can produce 4 moles of protons through its oxidation process (Equation 9) [5,23,48]. Pyrite is a common carrier of As and can also contain other metal(loid)s, such as Cu, Co, Ni, Pb, Sb and Zn. With the oxidation of pyrite, these potentially toxic elements can be liberated [49]. Based on the trends observed for the release of As, Fe and S in the resuspension experiment (Figure 2), it is likely that As is bound with pyrite. The trend can be observed for sample NC_2 (Figure 2), in which As, Fe and S all have an increased release around 200 days. With this release, there is also a rapid decrease in pH around 200 days, likely due to the dissolution of pyrite causing increased acidification (Figure 1). The decrease in As concentrations starting around 400 days (Figure 2) could be due to the oversaturation and thus precipitation with secondary minerals such as beudantite. Lead displays a different trend (Figure 2), in which there is some initial release, but then low to no release for the remaining 2 years. Thereby, Pb is likely not bound to pyrite. Lead minerals, such as galena or cerussite could be present in small concentrations (<0.5 wt%) in the original samples, and thus below the detection limit of XRD. In that case, Pb may have been initially released with the dissolution of a Pb-bearing mineral and then almost immediately precipitating as secondary Pb minerals such as plumbojarosite/beudantite.

There was a partial dissolution of pyrite in all samples except NC_1 after the 821-day resuspension experiment (<10 wt%; Table 1). Additionally, arsenopyrite and chalcopyrite completely dissolved after the 2-week and 821-day resuspension tests (sample FR_1, Table 1 and S1). This was partially confirmed by PHREEQC calculations, in which arsenopyrite completely dissolved and chalcopyrite partially dissolved by week 2. The saturation index of arsenopyrite was negative (SI=-22.6) and zero for chalcopyrite after 2 weeks.

One mole of pyrite exposed to molecular oxygen and water produces one mole of Fe(II), two moles of sulfate and two moles of H^+:

$$2FeS_2(s) + 7O_2 + 2H_2O \rightarrow 2Fe^{2+} + 4SO_4^{2-} + 4H^+ \quad (6)$$

In the presence of excess molecular oxygen (O_2), Fe(II) will subsequently oxidize to Fe(III) and consume one mole of H^+ [49] (Equation 7). This oxidation occurs rapidly at pH >4 or when catalyzed by bacterial activity [5], otherwise it occurs more slowly at lower pH values [50].

$$4Fe^{2+} + O_2 + 4H^+ \rightarrow 4Fe^{3+} + 2H_2O \quad (7)$$

The hydrolysis of Fe (III) promotes the precipitation of Fe(III) hydroxides and generates additional H^+:

$$Fe^{3+} + 3H_2O \rightleftharpoons Fe(OH)_3(s) + 3H^+ \quad (8)$$

Combining Equations 6-8 in Equation 9. Pyrite oxidizes in the presence of atmospheric oxygen and water, producing Fe(III) hydroxides, sulfate and 4 moles of protons per mole of pyrite oxidized by oxygen [5]:

$$4FeS_2 + 15O_2 + 14H_2O \rightarrow 4Fe(OH)_3 + 8SO_4^{2-} + 16H^+ \quad (9)$$

The production of Fe(III) hydroxides in the present study was seen with the formation of beudantite ($PbFe_3(OH)_6SO_4AsO_4$) and could potentially be a result of pyrite oxidation. However, the hydrolysis of Fe (III) (Equation 8) typically occurs at higher pH values (pH>5) [49], which was not the case in the resuspension tests performed in the present study (Figure 1).

Also, under acidic conditions (pH<3), Fe(III) can remain in solution and become the dominant oxidant [51]. This was also the case for a study by Lindsay et al. (2015). If pyrite is oxidized by Fe (III), 16 moles of H^+ are liberated:

$$FeS_2 + 14Fe^{3+} + 8H_2O \rightarrow 15Fe^{2+} + 2SO_4^{2-} + 16H^+ \quad (10)$$

Thereby, with these simplified reactions it is clear that even with partial oxidation of pyrite, as was seen in the present 821-day resuspension tests from most samples, there is still a high potential for acid generation. After 821 days of resuspension, the pyrite content decreased by 0, 10, 2 and 1 wt% for samples NC_1, NC_2, NC_3 and FR_1, respectively (Table 1). Samples NC_2 and NC_3 had the highest dissolution of pyrite (2-10 wt%) and the highest pH drop (resp. pH 5.4 $\rightarrow$1.7 and 6.1 $\rightarrow$ 2.13) by the end of the 821-day resuspension tests (Figure 1). Samples NC_1 and NC_3, with 0-1 wt% of pyrite dissolution, showed a lower decrease in pH by the end of the resuspension test: pH 4.9 to 2.5 and 3.5 to 2.02, respectively. These observations further confirm the influence of partial pyrite dissolution in the studied samples on acid generation.

Additionally, as some pyrite in the waste rock sample, NC_1 was found to be encapsulated in quartz (Supplementary Figure S1), upon further grinding of the material, the pyrite is likely liberated. In the environment, this decrease in particle size could occur via weathering/erosion or mechanically processing of mine waste to fine powder tailings, aiding in pyrite liberation and the potential subsequent increase in acid generation.

3.2.2 Reactivity of carbonate minerals

Siderite completely dissolved in all samples after 821 days of resuspension based on XRD analysis (Table 2), which can be expected because it is a fast-reacting mineral [52]. After the 2-week resuspension experiment of sample FR_1, the siderite concentration in the residue remained the same (original sample: 6 wt%; after 2-week resuspension: 7 wt%) (Supplementary Table S1). However, since siderite is a fast-reacting mineral, it likely did not take long after the 2-week resuspension experiment to dissolve. Other studies [53,54] have highlighted the precipitation and even oversaturation of siderite in AMD impacted aquifers. This can be due to the presence of ferrous iron in a carbonate-containing solution causing siderite to form via the following reaction [5]:

$$Fe^{2+} + HCO_3^- \rightleftharpoons FeCO_3 + H^+ \quad (11)$$

this buffers the reaction to around pH 5-5.5 [5]. The dissolution-oxidation reaction of siderite combined with ferrous iron oxidation and ferrihydrate formation is shown in Equation 12 [5]:

$$4FeCO_3 + O_2 + 10H_2O \rightleftharpoons 4HCO_3^- + 4Fe(OH)_3 + 4H^+ \quad (12)$$

This reaction indicates that under alkaline pH conditions where bicarbonate is stable, there is a net acid production of one mole of hydrogen together with the formation of ferrihydrate, whereas, under more acidic conditions, where carbonic acid is stable, there will be no net acid production [5]. The oxidation of pyrite

and siderite liberates Fe and SO_4^{2-} directly in solution, which may form secondary phases, such as beudantite or plumbojarosite [55]. Beudantite was found in samples NC_1, NC_2, and FR_1 after 821 days of resuspension (Table 1), in addition to the complete dissolution of siderite. This can be expected because the precipitation of Fe(III) (oxy)hydroxides and Fe(III) hydroxysulfates typically occurs within the oxidation zone, whereas hydrated Fe(II) sulfates tend to precipitate in water-unsaturated tailings below the oxidation zone [49]. The precipitation of beudantite with the oxidation of siderite was also observed in other studies (e.g., [55]). The PHREEQC calculations also indicated that the saturation index of beudantite was zero between pH 4.5 and 2, which also suggests the presence of beudantite in the residue.

In addition to siderite, other present carbonates or potential acid neutralizers consist of dolomite (FR_1, 4 wt%; Table 1) and hydrotalcite (1-3 wt% in all samples; Table 1). Based on PHREEQC calculations, dolomite and hydrotalcite start dissolving at pH<6. However, in comparison with the high content of acid-generating minerals, their neutralization seems almost negligible. Furthermore, the siderite (1-6 wt%) in the samples can also contribute to the acid generation over time or form secondary Fe(III) (oxy)hydroxide minerals (Equation 12). Nevertheless, over time the acid generated could react with the non-sulfidic gangue minerals, contributing to the acid neutralization. The most significant pH buffering reactions consist of the dissolution of carbonate minerals, aluminum hydroxide and Fe(III) hydroxide minerals and alumnosilicate minerals [24].

3.2.3 Low Pb release and formation of beudantite

The low concentrations of Pb leaching during the resuspension experiments can be explained by the complexation of Pb and precipitation of a newly formed Pb mineral, namely beudantite (Table 1). This theory is confirmed by the detection of beudantite in the residue via XRD analysis (Table 1; Supplementary Figures 10-13). The saturation indices of beudantite and plumbojarosite were calculated using PHREEQC. The saturation index of beudantite is zero, and it is negative for plumbojarosite (SI= approx. -24) between pH 4.5 and 2. Based on this calculation, beudantite is at equilibrium, which also suggests the presence of beudantite in the residues.

The formation of beudantite is commonly seen in acid-generating waters [55]. Furthermore, research also suggests that beudantite is stable under acidic conditions [42,43]. Courtin-Nomade et al. (2016) stated that in a supersaturated state, secondary phases may form and the predominant phases, plumbojarosite and beudantite are more stable and result in a limited release of As and Pb [55]. The latter was true in the current study for all samples. Maybe the dissolution of beudantite and plumbojarosite is kinetically driven and will also dissolve over an extended period. Field research has already shown that plumbojarosite can be replaced by other Pb-bearing minerals such as anglesite [56] and vice versa, indicating that Pb speciation and phases formed are strongly influenced by environmental conditions [44]. Additional field research, (e.g., [57]) detected beudantite in oxidized mine waste and stream sediments from samples taken from a historic mine in Cuba with acid pH effluents (active from 1980 to 1998). This could suggest the low solubility of beudantite in acidic conditions even over a longer period (>20 years). Also, Zhu et al. (2021) studied the long-term (330 days) dissolution and stability of beudantite and found that there was preferential detaching and solubility of sulfate and arsenate ions compared to Pb and Fe, which remained in the residue at an initial pH of 4 [58].

3.3 Kinetics of the pH-dependent leaching test and resuspension test

The results of the kinetic study of the pH-dependent leaching test are presented as the concentrations of elements leached as a function of pH (Figures 3) and as a function of time (Figure 4). In most cases, a shaking time of 24 h is sufficient to reach a steady state (Figures 3 and 4). Concerning pH, most elements

had a higher release under acidic conditions, which generally increased over time (Figure 3). In general, a longer shaking time (48 h) resulted in increased leaching of metal(loid)s; however, in some cases, such as between pH 2 and 5, a longer shaking time (48h) resulted in a decrease of Cu, Pb, Zn, Cd, S released. Generally, the longer the shaking time up to 24 h, the higher the release of metal(loid)s and sulfur, with some exceptions. For example, for extractions with pH 0.5, the Pb release decreased over time (2 to 24 h) and a steady state was reached at 24 h (Figure 4).

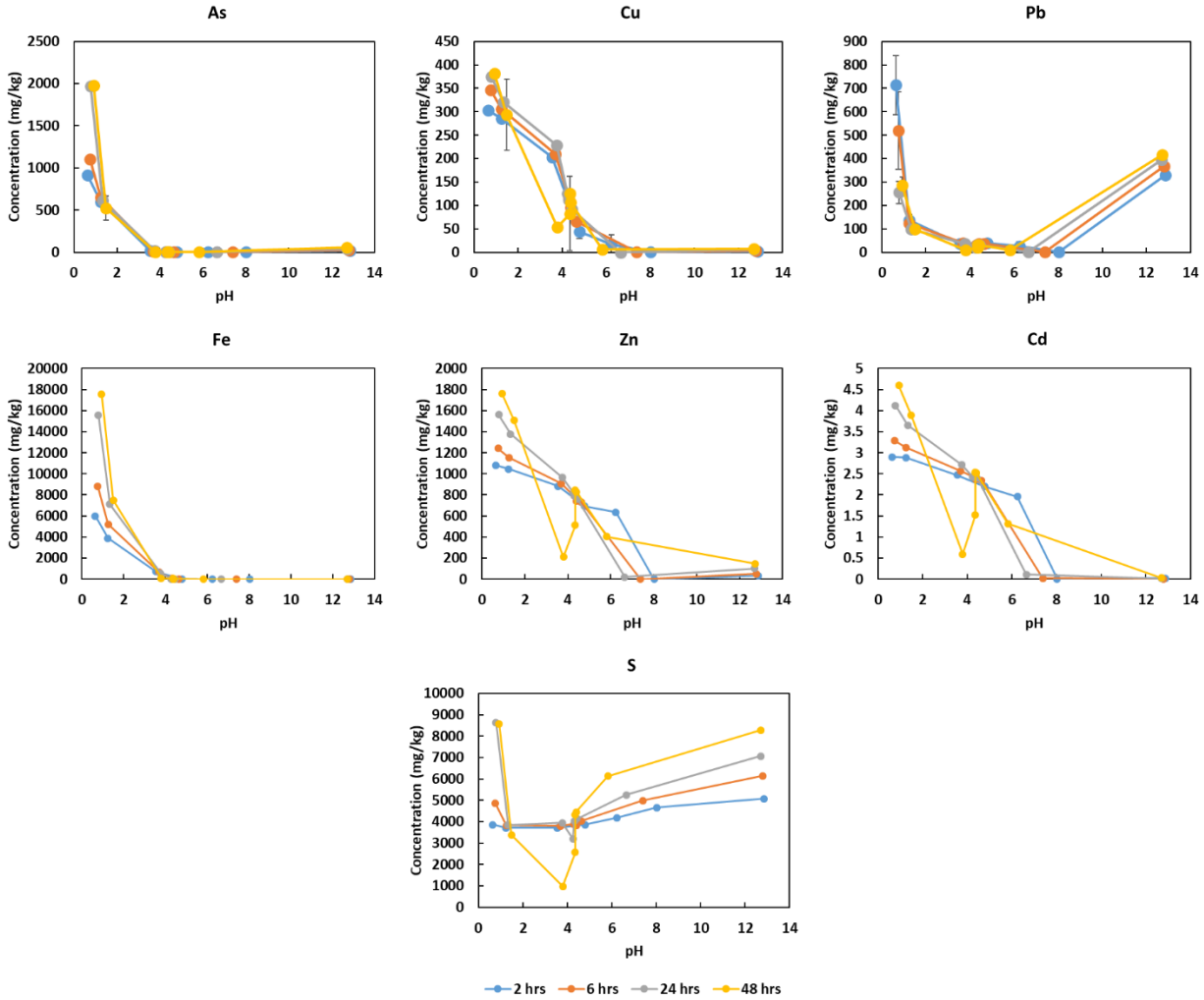

Figure 3 Comparison of pH-dependent leaching (pH from 0.5 to 13) at 4 different durations (2, 6, 24, and 48 h) for As, Cu, Pb, Fe, Zn, Cd, and S leached as a function of pH for sample NC_2. Error bars indicate standard deviation (n = 2). When error bars are not visible, they are smaller than the markers.

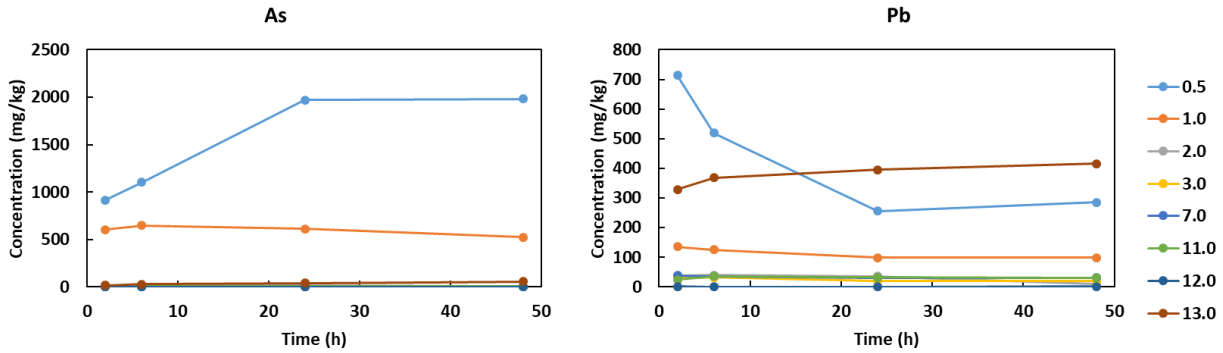

Figure 4 Comparison of pH-dependent leaching (from pH 0.5 to 13) at 4 different durations (2, 6, 24, and 48 h) for As and Pb leached as a function of time for sample NC_2.

The evaluation of time on the pH-dependent leaching further revealed the influence of kinetics on metal(loid) release. It appears that a steady state was reached at 24 h for most elements and thus a shaking period of 24 h could be sufficient, which is also in accordance with the US EPA's (2012) Method 1313. The release of Cu, Cd, Fe, Pb, Zn and S fluctuates between 2 and 48h, which is likely due to precipitation reactions. This phenomenon was also observed in a study by Cappuyns et al. (2014) [60].

Since pyrite remained in most of the mine waste residues after resuspension of 821 days, PHREEQC geochemical modeling was used to understand the longer-term (200 years) oxidation of pyrite within the studied samples under similar conditions. The kinetic geochemical modeling revealed that a steady-state would be reached within the first four months under similar oxidizing conditions as the resuspension experiment. For sample NC_2, the pH evolved from pH 5.4 and stabilized to a pH of around 3.5 until 200 years. The other samples had a similar pH evolution, starting from the original pH of the resuspension test. However, this model is an oversimplification and other factors can play a role in the oxidation of pyrite (e.g., the influence of other minerals or organic matter). Thereby, experimental testing is crucial given the differences between the model and the experimental resuspension tests.

3.4 Static ABA results compared with long-term kinetic resuspension test

The NNP values from both the laboratory experiments (EN 15875 test) and the theoretical calculations were all <-20 kg/t, meaning that the samples have a high acid generation potential (Table 2).

Table 2 The experimental and theoretical net neutralization potential (NNP) of each sample.

	Experimental	**Theoretical** (XRD mineralogy results)
Sample code	**NNP** ($CaCO_3$ equivalent in kg/t)	**NNP** ($CaCO_3$ equivalent in kg/t)
NC_1	-192	-80
NC_2	-688	-573
NC_3	-124	-38
FR_1	-309	-203

Reference	EN 15875, 2011 [17]	Dold, 2017 [5]

While static ABA tests, such as the EN 15875 test, are used to predict if a sample has the potential to acidify the geochemical system, kinetic testing is used to investigate in which time frame this will occur [5].

For the static ABA test, a NNP value <-20kg/t $CaCO_3$ indicates that the material is acid-producing. According to the results (Table 2), all samples are well below -20 kg/t $CaCO_3$ and are therefore highly acid-producing. The main acid-generating mineral in the samples was pyrite. Tailings samples NC_2 and FR_1 had the highest content of pyrite (Table 1; 35 and 13 wt%, respectively); which explains why they have the lowest experimental and theoretical NNP values (Table 2; -688 and -309 kg/t $CaCO_3$, respectively).

The initial pH of the mine waste samples during the resuspension tests ranged from pH 3.5-6.1, with the following sample order: FR_1<NC_1<NC_2<NC_3. After the 821-day resuspension tests, the pH dropped to pH 1.7-2.5 with a change in sample order: NC_2<FR_1< NC_3<NC_1. The predicted acid generation potential based on standard method EN 15875 and theoretical calculation (based on mineralogy) was almost in agreement with the order of samples based on the pH drop: NC_2<FR_1< NC_1<NC_3. This order of samples based on the static tests and calculations is in agreement with the pyrite content of each sample NC_2 (35 wt%) >FR_1 (13 wt%) >NC_1 (5 wt%) >NC_3 (2 wt%) (Table 1). The reason for the difference in sample order between the resuspension test and the static ABA tests is that the static tests consider the full dissolution of pyrite. However, as was observed in the kinetic resuspension experiment, pyrite only partially dissolved or did not dissolve at all in most samples.

Sample NC_3 started with the highest pH (pH 6.1 at t=0 days) but decreased significantly to pH 2.1 by day 821 of the resuspension test. In comparison with the other waste rock sample, NC_1, which had a lower starting pH (pH 5.9 at t=0 days), but had a smaller drop in pH, to pH 2.5 by day 821. The larger decrease in pH during the 821-day resuspension experiment for the oxidized waste rock (NC_3) compared to the fresh waste rock (NC_1) samples can be explained by the greater oxidation of pyrite in the resuspended residue from sample NC_3 (Table 1). Sample NC_3 had a decrease of 2 wt% of pyrite, whereas for sample NC_1 there was no decrease in pyrite content over 821 days.

This overestimation of the acid generation potential of sulfidic mine waste samples from static ABA tests has been reported in other studies (e.g., [4,5]). The present research is one of the first studies to perform such a long-term kinetic experiment in comparison with an ABA test. While it is clear that static ABA tests like the EN 15875 provide initial insights into the acid generation potential of the samples, it is still necessary to perform kinetic experiments, such as the resuspension test or in situ measurements over an extended period for a more realistic understanding, especially for mine waste with complex mineralogy.

3.5 Practical implications and potential management scenarios

The mine tailings and waste rock from the mining sites in both Neves-Corvo and Freiberg were characterized by a high acid generation potential as well as the high mobility of potentially toxic elements such as As, Cd, Cu and Zn. As a result, the investigated mine waste likely poses high environmental and human health risks. Neves-Corvo mine is currently an operational mine and thus these wastes are currently being monitored and managed. Since 2010, thickened tailings are disposed of in a sub-aerial tailings dam onsite in a co-deposition system contained with berms built with waste rock, and the waste rock is stored temporarily in a stockpile [41]. Based on the current study, it is clear that the mine tailings and waste rock still contain high and mobile levels of metal(loid)s, including valuable metals (e.g., Cu and Zn), and thereby

have the potential for valorization. It could be useful to combine a metal(loid) recovery/cleaning method to the tailings and waste rock with a valorization process of incorporating the residues (remaining after removal of the valuable metals) in building materials. For example, a study by Niu et al. (2021) has investigated the successful use of mechanochemical activation of the Neves-Corvo waste rock in the fabrication of inorganic polymers [61].

The FR_1 tailings sample is from an abandoned tailings impoundment in the Freiberg mining district. Based on the results from the present study, it is encouraged for these tailings to be managed due to the high acid generation potential and high release of potentially toxic elements that can easily make their way into the waterways on-site and surrounding areas. Other studies [62,63] have already highlighted the contamination recorded from the stored tailings in the Freiberg mining district. For example, GEOS, (2012) reported particularly high Cd levels in the Freiberger Mulde river, which they traced to the water seepage from the tailings layers and dam walls; the contaminated water laden with Cd made its way into the groundwater and channeled through the old mine tunnels and to the river [62]. Similar to the Neves-Corvo tailings, the high content of metal(loid)s makes these tailings potentially suitable for recovery approaches (e.g., flotation or bioleaching). Additionally, to mitigate the environmental risks on-site, in situ methods could be applied. For example, the method of phytostabilization can be considered to eliminate areas of exposed tailings [64,65].

4. Conclusion

This study aimed to determine the acid generation potential and consequent metal(loid) release from mine waste through geochemical, static, kinetic and mineralogical characterizations to understand the underlying drivers (e.g., mineralogy, kinetics, and pH) for acid production and metal(loid) release.

Overall, there were high levels of contaminants released (e.g., As, Cd, Cu, and Zn) and the mine waste showed a high acid generation potential during the resuspension tests. The decrease in pH and increase in metal(loid) release was also generally more pronounced over time. However, low levels of Pb were released, which can be attributed to the precipitation of secondary Pb-minerals such as beudantite. The precipitation of beudantite was confirmed by mineralogical analysis and PHREEQC calculations. Experimental and calculated NNP values were negative in all cases, suggesting the high acid generation potential, which is in agreement with the kinetic leaching test and modeling. Static tests and theoretical calculations based on the mineralogy are useful in understanding sample characteristics; however, they should not be used as standalone methods. The current study revealed the importance of kinetic testing due to geochemical behaviors which are not linear with time and are challenging to model. While it is clear that kinetic laboratory testing is important, comparison with field tests is also crucial.

These results were important in understanding the characteristics of the mine waste, especially over the long term, to highlight potential remediation options and at the same time compare different methods of determining the acid generation potential and role of kinetics. This study revealed that the studied mine wastes can be detrimental to the environment and thus appropriate management scenarios should be implemented. One option could be the recovery of valuable metals and the removal of hazardous metals using different technologies such as bioleaching and ion flotation methods. The residue could then be incorporated into construction materials to increase pH, e.g., inorganic polymers and cements. An environmental assessment of the output of these valorized products will be investigated in future research.

Acknowledgments

This work has received funding from the European Union's EU Framework Program for Research and Innovation Horizon 2020 Grant Agreement No. 812580 (MSCA-ETN SULTAN). The authors would like to thank Alexandra Gomez Escobar, Prof. Jorge Relvas, Mafalda Oliveira, Álvaro Pinto, Rosie Blannin, and Dr. Max Frenzel for the collection and distribution of the samples from Neves-Corvo and Freiberg and the provision of site and sample information. We are also grateful for Elvira Vassilieva's and Nancy Weyns' assistance with instrumental analyses. The authors would also like to thank Herman Nijs for the preparation of the polished sections and Ana Lupu for carrying out the SEM analyses. We also thank the anonymous reviewers and editor for their valuable comments and time.

References

[1] B.G. Lottermoser, Mine wastes-characterization, treatment, environmental impacts, 2nd ed., Springer, Berlin, Germany, 2007.

[2] M. Becker, N. Dyantyi, J.L. Broadhurst, S.T.L. Harrison, J.-P. Franzidis, A mineralogical approach to evaluating laboratory scale acid rock drainage characterisation tests, Miner. Eng. 80 (2015) 33–36. https://doi.org/10.1016/j.mineng.2015.06.015.

[3] D.W. Blowes, J.L. Jambor, C.N. Alpers, Acid-neutralization mechanisms in inactive mine tailings, in: Environ. Geochemistry Sulfide Mine Wastes, Mineralogical Association of Canada, Ontario, Canada, 1994: pp. 95–116.

[4] T. Karlsson, M.L. Räisänen, M. Lehtonen, L. Alakangas, Comparison of static and mineralogical ARD prediction methods in the Nordic environment, Environ. Monit. Assess. 190 (2018). https://doi.org/10.1007/s10661-018-7096-2.

[5] B. Dold, Acid rock drainage prediction: A critical review, J. Geochemical Explor. 172 (2017) 120–132. https://doi.org/10.1016/j.gexplo.2016.09.014.

[6] W. Zhang, L. Alakangas, Z. Wei, J. Long, Geochemical evaluation of heavy metal migration in Pb-Zn tailings covered by different topsoils, J. Geochemical Explor. 165 (2016) 134–142. https://doi.org/10.1016/j.gexplo.2016.03.010.

[7] J. Lu, L. Alakangas, Y. Jia, J. Gotthardsson, Evaluation of the application of dry covers over carbonate-rich sulphide tailings, J. Hazard. Mater. 244–245 (2013) 180–194. https://doi.org/10.1016/j.jhazmat.2012.11.030.

[8] E.K. Yanful, A. Verma, Oxidation of flooded mine tailings due to resuspension, Can. Geotech. J. 36 (1999) 826–845. https://doi.org/10.1139/t99-044.

[9] L.T. Nguyen, Mobilization of metals from mining wastes and the resuspension of contaminated sediments, Linkoping University in Arts and Sciences.430, 2008.

[10] C. Adu-Wusu, E.K. Yanful, M.H. Mian, Field evidence of resuspension in a mine tailings pond, Can. Geotech. J. 38 (2001) 796–808. https://doi.org/10.1139/t01-005.

[11] A.S. Awoh, M. Mbonimpa, B. Bussière, B. Plante, H. Bouzahzah, Laboratory study of highly pyritic tailings submerged beneath a water cover under various hydrodynamic conditions, Mine Water Environ. 33 (2014) 241–255. https://doi.org/10.1007/s10230-014-0264-x.

[12] V. Cappuyns, R. Swennen, A. Devivier, Dredged river sediments: Potential chemical time bombs? A case study, Water. Air. Soil Pollut. 171 (2006) 49–66. https://doi.org/10.1007/s11270-005-9012-y.

[13] V. Ettler, Z. Johan, 12years of leaching of contaminants from Pb smelter slags: Geochemical/mineralogical controls and slag recycling potential, Appl. Geochemistry. 40 (2014) 97–103. https://doi.org/10.1016/j.apgeochem.2013.11.001.

[14] A.A. Sobek, W.A. Schuller, J.R. Freeman, R.M. Smith, Field and laboratory methods applicable to overburdens and Minesoils EPA-600/2-78-054, Washington, DC, 1978. https://cfpub.epa.gov/si/si_public_record_Report.cfm?Lab=ORD&dirEntryID=44259.

[15] R.W. Lawrence, G.W. Poling, G.M. Ritcey, P.B. Marchant, Assessment of predictive methods for the determination of AMD potential in mine tailings and waste rock, tailings and effluent management, Pergamon Press, Elmsford, NY, USA, 1989.

[16] R.W. Lawrence, Y. Wang, Determination of neutralization potential in the prediction of acid rock drainage, in: 4th Int. Conf. Acid Rock Drain., Vancouver, BC, 1997: pp. 449–464.

[17] EN 15875, Characterization of waste-Static test for determination of acid potential and neutralization potential of sulfidic waste, 2011.

[18] H.A. van der Sloot, A. van Zomeren, Characterisation leaching tests and associated geochemical speciation modelling to assess long term release behaviour from extractive wastes, Mine Water Environ. 31 (2012) 92–103. https://doi.org/10.1007/s10230-012-0182-8.

[19] O.A. Abegunde, C. Okujeni, L. Petrik, A.M. Siad, G. Madzivire, C. Wu, The use of factor analysis and acid base accounting to probe the speciation of toxic metals in gold mine waste, Environ. Earth Sci. 79 (2020) 1–13. https://doi.org/10.1007/s12665-020-8887-7.

[20] R.W. Lawrence, M. Scheske, A method to calculate the neutralization potential of mining wastes, Environ. Geol. 32 (1997) 100–106. https://doi.org/10.1007/s002540050198.

[21] H.E. Jamieson, S.R. Walker, M.B. Parsons, Mineralogical characterization of mine waste, Appl. Geochemistry. 57 (2015) 85–105. https://doi.org/10.1016/j.apgeochem.2014.12.014.

[22] A. Parbhakar-Fox, B.G. Lottermoser, A critical review of acid rock drainage prediction methods and practices, Miner. Eng. 82 (2015) 107–124. https://doi.org/10.1016/j.mineng.2015.03.015.

[23] D.K. Nordstrom, Advances in the Hydrogeochemistry and Microbiology of Acid Mine Waters, Int. Geol. Rev. 42 (2000) 499–515. https://doi.org/10.1080/00206810009465095.

[24] D.W. Blowes, C.J. Ptacek, J.L. Jambor, C.G. Weisener, D. Paktunc, W.D. Gould, D.B. Johnson, The geochemistry of acid mine drainage, 2nd ed., Elsevier, Oxford, UK, 2014.

[25] K.D. Ferguson, P.M. Erickson, Pre-mine prediction of acid mine drainage, in: W. In Salomons, U. Förstner (Eds.), Environ. Manag. Solid Wastes Dredged Mater. Mine Tailings, Springer-Verlarg, Berlin Heidelberg, 1988: pp. 24–43. https://doi.org/10.1007/978-3-642-61362-3_2.

[26] N. Seignez, A. Gauthier, D. Bulteel, D. Damidot, J. Potdevin, Applied Geochemistry Leaching of lead metallurgical slags and pollutant mobility far from equilibrium conditions, Appl.

Geochemistry. 23 (2008) 3699–3711. https://doi.org/10.1016/j.apgeochem.2008.09.009.

[27] R. Barna, P. Moszkowicz, C. Gervais, Leaching assessment of road materials containing primary lead and zinc slags, Waste Manag. 24 (2004) 945–955. https://doi.org/10.1016/j.wasman.2004.07.014.

[28] J. Helser, E. Vassilieva, V. Cappuyns, Environmental and Human Health Risk Assessment of Sulfidic Mine Waste: Bioaccessibility, Leaching and Mineralogy, J. Hazard. Mater. 424 (2022). https://doi.org/10.1016/j.jhazmat.2021.127313.

[29] ISO 11465, Soil quality — Determination of dry matter and water content on a mass basis — Gravimetric method, Geneva (Switzerland), 1993. https://www.iso.org/standard/20886.html.

[30] J. Bergmann, P. Friedel, R. Kleeberg, BGMN - a New Fundamental Parameters Based Rietveld Program for Laboratory X-ray Sources, it's Use in Quantitative Analysis and Structure Investigations, IUCr Comm. Powder Diffr. Newsl. 20 (1998) 5–8.

[31] R. Snellings, L. Machiels, G. Mertens, J. Elsen, Rietveld refinement strategy for quantitative phase analysis of partially amorphous zeolitized tuffaceous rocks, Geol. Belgica. 13 (2010) 183–196.

[32] J. Helser, A. Lupu, V. Cappuyns, Acid generation potential and metal(loid) release from resuspended sulfidic mine waste, Abstract, in: Goldschmidt Conf., 2021.

[33] M.H. Larsen, K. Biermann, S. Tandberg, T. Hsu, J. Jacobs, W.R., Genetic manipulation of Mycobacterium tuberculosis, Curr. Protoc. Microbiol. 10 (2007). https://doi.org/10.1002/9780471729259.mc10a02s6.

[34] D.L. Parkhurst, C.A.J. Appelo, User's guide to PHREEQC (version 3) – a computer program for speciation, batch-reaction, one-dimensional transport and inverse geochemical calculations., (1999).

[35] M.A. Williamson, J.D. Rimstidt, The kinetics and electrochemical rate-determining step of aqueous pyrite oxidation, Geochim. Cosmochim. Acta. 58 (1994) 5443–5454.

[36] C.A.J. Appelo, D. Postma, Geochemistry, Groundwater and Pollution, 2nd ed., CRC Press, 2005. https://doi.org/https://doi.org/10.1201/9781439833544.

[37] L.E. Eary, M.A. Williamson, Simulations of the neutralizing capacity of silicate rocks in acid mine drainage environments, 7th Int. Conf. Acid Rock Drain. 2006, ICARD - Also Serves as 23rd Annu. Meet. Am. Soc. Min. Reclam. 1 (2006) 564–577. https://doi.org/10.21000/jasmr06020564.

[38] B.M. Chapman, D.R. Jones, R.F. Jung, Processes controlling metal ion attenuation in acid mine drainage streams, Geochim. Cosmochim. Acta. 47 (1983) 1957–1973. https://doi.org/10.1016/0016-7037(83)90213-2.

[39] C. Roussel, C. Néel, H. Bril, Minerals controlling arsenic and lead solubility in an abandoned gold mine tailings, Sci. Total Environ. 263 (2000) 209–219. https://doi.org/10.1016/S0048-9697(00)00707-5.

[40] D. Bendz, C. Tiberg, D.B. Kleja, Mineralogical characterization and speciation of sulfur, zinc and lead in pyrite cinder from Bergvik, Sweden, Appl. Geochemistry. 131 (2021) 105010.

https://doi.org/10.1016/j.apgeochem.2021.105010.

[41] A.G. Escobar, J.M.R.S. Relvas, Á.M.M. Pinto, M. Oliveira, Physical–chemical characterization of the Neves Corvo extractive mine residues: A perspective towards future mining and reprocessing of sulfidic tailings, J. Sustain. Metall. (2021). https://doi.org/10.1007/s40831-021-00428-1.

[42] J. Helser, V. Cappuyns, Trace elements leaching from Pb-Zn mine waste (Plombières, Belgium) and environmental implications, J. Geochemical Explor. 220 (2021). https://doi.org/10.1016/j.gexplo.2020.106659.

[43] A. Courtin-Nomade, C. Neel, H. Bril, M. Davranche, Trapping and mobilisation of arsenic and lead in former mine tailings –Environmental conditions effects, Bull. La Société Géologique Fr. 173 (2002) 479–485. https://doi.org/10.2113/173.5.479.

[44] F.L. Forray, A.M.L. Smith, C. Drouet, A. Navrotsky, K. Wright, K.A. Hudson-Edwards, W.E. Dubbin, Synthesis, characterization and thermochemistry of a Pb-jarosite, Geochim. Cosmochim. Acta. 74 (2010) 215–224. https://doi.org/10.1016/j.gca.2009.09.033.

[45] A.P. Chung, C. Coimbra, P. Farias, R. Francisco, R. Branco, F. V. Simão, E. Gomes, A. Pereira, M.C. Vila, A. Fiúza, M.S. Mortensen, S.J. Sørensen, P. V. Morais, Tailings microbial community profile and prediction of its functionality in basins of tungsten mine, Sci. Rep. 9 (2019) 1–13. https://doi.org/10.1038/s41598-019-55706-6.

[46] T. Natal da Luz, R. Ribeiro, J.P. Sousa, Avoidance tests with Collembola and Earthworms as early screening tools for site-specific assessment of polluted soils, Environ. Toxicol. Chem. 23 (2004) 2188–2193. https://doi.org/10.1897/03-445.

[47] K. Ciarkowska, E. Hanus-Fajerska, F. Gambuś, E. Muszyńska, T. Czech, Phytostabilization of Zn-Pb ore flotation tailings with Dianthus carthusianorum and Biscutella laevigata after amending with mineral fertilizers or sewage sludge, J. Environ. Manage. 189 (2017) 75–83. https://doi.org/10.1016/j.jenvman.2016.12.028.

[48] B. Dold, Evolution of acid mine drainage formation in sulphidic mine tailings, Minerals. 4 (2014) 621–641. https://doi.org/10.3390/min4030621.

[49] M.B.J. Lindsay, M.C. Moncur, J.G. Bain, J.L. Jambor, C.J. Ptacek, D.W. Blowes, Geochemical and mineralogical aspects of sulfide mine tailings, Appl. Geochemistry. 57 (2015) 157–177. https://doi.org/10.1016/j.apgeochem.2015.01.009.

[50] US Environmental Protection Agency, Acid Mine Drainage Prediction, 1994. https://19january2017snapshot.epa.gov/sites/production/files/2015-09/documents/amd.pdf.

[51] P.C. Singer, W. Stumm, Acid mine drainage-rate determining step, Science (80-.). 167 (1970) 1121–1123. https://doi.org/10.1126/science.167.3921.1121.

[52] J. Bundschuh, M. Zilberbrand, Geochemical modeling of groundwater, vadose and geothermal systems, 1st ed., Ringgold, Inc, 2011. http://urn.kb.se/resolve?urn=urn:nbn:se:kth:diva-246966.

[53] K.A. Morin, J.A. Cherry, Trace amounts of siderite near a uranium-tailings impoundment, Elliot Lake, Ontario, Canada, and its implication in controlling contaminant migration in a sand aquifer, Chem. Geol. 56 (1986) 117–134. https://doi.org/10.1016/0009-2541(86)90115-4.

[54] B. Dold, C. Wade, L. Fontboté, Water management for acid mine drainage control at the polymetallic Zn-Pb-(Ag-Bi-Cu) deposit Cerro de Pasco, Peru, J. Geochemical Explor. 100 (2009) 133–141. https://doi.org/10.1016/j.gexplo.2008.05.002.

[55] A. Courtin-Nomade, T. Waltzing, C. Evrard, M. Soubrand, J.-F. Lenain, E. Ducloux, S. Ghorbel, C. Grosbois, H. Bril, Arsenic and lead mobility: From tailing materials to the aqueous compartment, Appl. Geochemistry. 64 (2016) 10–21. https://doi.org/10.1016/j.apgeochem.2015.11.002.

[56] M.I. Leybourne, J.M. Peter, D. Layton-Matthews, J. Volesky, D.R. Boyle, Mobility and fractionation of rare earth elements during supergene weathering and gossan formation and chemical modification of massive sulfide gossan, Geochim. Cosmochim. Acta. 70 (2006) 1097–1112. https://doi.org/10.1016/j.gca.2005.11.003.

[57] F.M. Romero, R.M. Prol-Ledesma, C. Canet, L.N. Alvares, R. Pérez-Vázquez, Acid drainage at the inactive Santa Lucia mine, western Cuba: Natural attenuation of arsenic, barium and lead, and geochemical behavior of rare earth elements, Appl. Geochemistry. 25 (2010) 716–727. https://doi.org/10.1016/j.apgeochem.2010.02.004.

[58] Y. Zhu, W. Wei, S. Tang, Z. Zhu, Q. Yan, L. Zhang, H. Deng, A comparative study on the dissolution and stability of beudantite and hidalgoite at pH 2–12 and 25–45°C for the possible long-term simultaneous immobilization of arsenic and lead, Chemosphere. 263 (2021). https://doi.org/10.1016/j.chemosphere.2020.128386.

[59] US EPA, Method 1313 Liquid-solid partitioning as a function of extract pH using a parallel batch extraction procedure, 14429 (2012) 57–77.

[60] V. Cappuyns, V. Alian, E. Vassilieva, R. Swennen, pH dependent leaching behavior of Zn, Cd, Pb, Cu and As from mining wastes and slags: Kinetics and mineralogical control, Waste and Biomass Valorization. 5 (2014) 355–368. https://doi.org/10.1007/s12649-013-9274-3.

[61] H. Niu, L. Raka, A. Alexandra, G. Escobar, V. Zhukov, P. Perumal, Potential of Mechanochemically Activated Sulfidic Mining Waste Rock for Alkali Activation, J. Sustain. Metall. (2021). https://doi.org/10.1007/s40831-021-00466-9.

[62] GEOS, Detailuntersuchung des wasserpfades am object spülhalde Davidschacht, Halsbrücke, 2012.

[63] E. Fritz, C. Jahns, Die Spülhalde Davidschacht in Freiberg – Geschichte, Umweltproblematik und geplante Sanierung: The flotation taining “Davidschacht” in Freiberg-history, environmental problems and planned remediation, 2 (2017) 4–17.

[64] O. Karaca, C. Cameselle, K.R. Reddy, Mine tailing disposal sites: contamination problems, remedial options and phytocaps for sustainable remediation, Rev. Environ. Sci. Biotechnol. 17 (2018) 205–228. https://doi.org/10.1007/s11157-017-9453-y.

[65] J. Gil-Loaiza, S.A. White, R.A. Root, F.A. Solís-Dominguez, C.M. Hammond, J. Chorover, R.M. Maier, Phytostabilization of mine tailings using compost-assisted direct planting: Translating greenhouse results to the field, Sci. Total Environ. 565 (2016) 451–461. https://doi.org/10.1016/j.scitotenv.2016.04.168.